

# Testing time evolution of the mass distribution of the black hole mergers

So Okano<sup>1</sup>, Teruaki Suyama<sup>1</sup>

<sup>1</sup>*Department of Physics, Tokyo Institute of Technology, 2-12-1 Ookayama, Meguro-ku, Tokyo 152-8551, Japan*

## Abstract

Detection of the gravitational-wave events revealed that there are numerous population of the black hole binaries which can merge within the age of the Universe. Although several formation channels of such binaries are known, considerable theoretical uncertainties associated in each channel defeats the robust prediction of how much each channel contributes to the total merger rate density. Given that the time evolution of the merger rate density in some channels is (exactly or nearly) independent of the BH masses, clarifying this feature from the observational data will shed some light on the nature of the black hole binaries. Based on this motivation, we formulate the methodology to perform the statistical test of whether the mass distribution of the black hole mergers evolves in time or not by means of the hypothesis testing. Our statistical test requires neither a priori specification of the mass distribution which is largely uncertain nor that of the time dependence of the merger rate. We then apply it to the mock data for some concrete shapes of the merger rate density and show that the proposed method rejects/(does not reject) the null hypothesis correctly for the large sample size. We also investigate if the catalog of the gravitational-wave events obtained during the LIGO-Virgo's third observing run has a large sample size enough to apply our hypothesis testing. We find that the number of the events is too small to draw any statistical conclusion regarding our test and the meaningful result of our hypothesis testing can be obtained only by the future detectors having much better sensitivity. These results demonstrate the effectiveness of our hypothesis testing to determine from the (future) observational data whether the merger rate density evolves in time independently of the BH masses or not.

## 1 Introduction

Detection of gravitational waves from the mergers of black holes (BHs) has revealed numerous population of BH binaries in the Universe [1, 2]. Several formation channels have

been proposed to explain the origin of such BH binaries (e.g., see [3, 4]). Astrophysically, binary BHs can be directly formed as the end product of the stellar evolution of the field binary. As another formation channel, individual BHs formed in dense environment can later form binaries dynamically. Exhaustive summary of the astrophysical scenarios for the formation of the BH binaries and their mergers as well as the expected merger rate in each scenario are found in [5]. It is also possible that BHs that might have been created right after the BigBang (so-called primordial BHs) form binaries in the radiation dominated epoch and become the source of the detected GWs. Yet, it is not clear if the current data favors the existence of the PBHs [6].

Because of the considerable theoretical uncertainties in each channel, it is still unknown how much each formation scenario contributes to the merger rate [7]. Conversely, we may give feedback to these theoretical models and update them from observational data whose information in terms of the merger rate, redshift, mass distribution, spin, etc. has been increasing and will continue to increase in the future due to the progress of the GW detectors. Along this path, one of the attempts we could do is to elucidate if a single channel dominates the observed merger events or a few different channels nearly equally contribute. To this end, we focus on the particular type of the merger rate density written as

$$\mathcal{R}(m_1, m_2, t) = \mathcal{R}_0 h(m_1, m_2) f(t). \quad (1.1)$$

Here  $m_1, m_2$  are the mass of individual BH in the binary measured in the source frame, and  $t$  is the cosmic age when the merger occurred.  $h(m_1, m_2)$  is normalized such that  $\int h(m_1, m_2) dm_1 dm_2 = 1$  and  $f(t)$  is normalized such that  $f(t_0) = 1$ , where  $t_0$  is the age of the Universe. Thus,  $\mathcal{R}_0$  represents the merger rate at present time. Dimension of  $\mathcal{R}$  is  $/\text{Gpc}^3/\text{yr}/M_\odot^2$ , and the rate density is defined for the comoving volume and the cosmic time. Thus,  $\mathcal{R}(m_1, m_2, t) dV_c dt dm_1 dm_2$  represents the number of the merger events of BHs with masses  $m_1, m_2$  that happen in the comoving volume  $dV_c$  and during the time interval  $(t, t + dt)$ .

A crucial property of the merger rate density above is that the dependence on the BH mass and that on the merger time (i.e., redshift) are separated: it is simply given by the product of the mass-dependent function and the time-dependent function. In other words, the mass distribution of the merger rate density does not evolve in time. Whether such evolution occurs or not depends on the formation channels. In the isolated field binary scenario, the merger rate density is given by the convolution of the star formation rate and the merger time delay distribution [8]. Both of these may depend on the binary masses, and the resultant merger rate density exhibits time evolution of the mass distribution [9, 10]. For the mergers in globular clusters, the merger rate is given by the convolution of the globular cluster formation rate and the merger time delay distribution [11]. Time-dependence of the mass distribution is determined by whether the mergers are dominated by the binaries ejected from the globular cluster or the binaries that remain inside until they merge. In the former case, ejection efficiency depends on the BH masses, which yields the time dependent mass distribution [12]. On the other hand, if the latter case is the dominant process, mergers follow shortly after the BH-BH

encounter [13] and the time evolution of the mass distribution will be suppressed [14]. As another merger channel, BH-BH encounters in the galactic nuclei [15–17] may be expected to have very little time evolution of their mass distribution [18, 19], similarly to the single-single GW captures in globular clusters [14]. Meanwhile, in the primordial BH scenario, the mass distribution remains almost constant in time [20, 21].

Since each channel has different time evolution and mass distribution, the total merger rate density will not take the separable form (1.1) in general. Thus, an observational confirmation of the time independence of the mass distribution will support the idea that some single channel is dominating the merger events. On the other hand, confirmation of the opposite case does not necessary imply the contribution of the multiple channels. In the latter case, more detailed investigations on the time evolution of the mass distribution or use of other quantities will be required to extract information on the channels. Anyway, this consideration motivates us to take an agnostic point of view on the dominant channels of the BH mergers and to test if the merger rate density obeys the separable form by making comparison with observational data <sup>#1</sup>. Although the current data, due to the limited number of the merger events, is not enough to conduct this program (see Sec. 3.4), given the promised progress of the GW observations, much more merger events detected in the future will enable us to successfully test the hypothesis.

In light of this, our aim is to formulate the statistical method to test whether the observed merger rate density obeys the form (1.1) or not <sup>#2</sup>. As we will demonstrate, our method does not assume a priori the functional shape of  $h(m_1, m_2)$  and  $f(t)$  both of which strongly depend on the formation channel as well as the underlying assumptions. Thus, our method can be used without making a particular assumption on those functions. Before concluding this section, let us mention that [23] also studied the time evolution of the mass distribution. In that paper, time variation of the upper cutoff of the BH mass is considered as a crucial quantity to represent the time evolution of the mass distribution, and the approach is not the same as what we will develop in the following.

## 2 Formulation of the method

For convenience, instead of the masses of the individual BHs and the cosmic merger time, we will use the total mass  $M = m_1 + m_2$ , the mass ratio  $q = \frac{m_2}{m_1} (m_2 \leq m_1)$ , and the redshift  $z$  in the following analysis. In terms of the new variables, the expected number of the merger events in the small mass area  $dM dq$  and the redshift bin  $(z, z + dz)$  during the observation time  $T$  is given by

$$dN = \mathcal{R}(M, q, z) \frac{T}{1+z} \frac{4\pi r^2(z) dz}{H(z)} \frac{M}{(1+q)^2} dM dq. \quad (2.1)$$

---

<sup>#1</sup>In [22], the merger rate density taking the separable form with some specific functional shapes was confronted with the early LIGO-Virgo data.

<sup>#2</sup>As for the total merger rate  $\int \mathcal{R} dm_1 dm_2$ , there is a strong support for the increase toward the higher redshift [23, 24].

Here  $\frac{T}{1+z}$  is the time interval corresponding to  $T$  in the source frame,  $r(z)$  is the comoving distance to the redshift  $z$ ,  $dV_c = \frac{4\pi r^2(z)}{H(z)} dz$  is the comoving volume of the thin shell ( $z, z + dz$ ), and  $\frac{M}{(1+q)^2}$  is the Jacobian due to the transformation from  $(m_1, m_2)$  to  $(M, q)$ . Notice that the separability of the mass dependence and the merger time dependence which  $\mathcal{R}$  possesses (i.e., Eq. (1.1)) is retained by  $dN$ , which plays a crucial role in the following analysis.

The number of the events given above does not take into account the selection bias of the detector which becomes important for region in the  $(M, q, z)$  space close to and beyond the detection horizon. This effect can be included by multiplying the detection probability  $p_{\text{det}}(M, q, z)$ , which is the probability that a given detector (or a network of detectors) detects the merger event with masses  $(M, q)$  occurring at  $z$ , on the right-hand side of Eq. (2.1). Concrete shape of  $p_{\text{det}}$  depends on the detector (or a network of detectors) [25]. Since  $p_{\text{det}}$  does not take the separable form in general, inclusion of the events corresponding to  $p_{\text{det}} < 1$  invalidates the separability ansatz for  $dN$ . In the following analysis, we assume an ideal case  $p_{\text{det}} = 1$  or equivalently consider only events much within the detection horizon. In Sec. 3.4, we briefly discuss how much the selection bias affects the performance of our method.

## 2.1 Basic idea

Let us take two distinct closed regions in the two-dimensional mass plane spanned by  $(M, q)$  (Region 1 and region 2 in Fig. 1) and two intervals  $(z_a, z_b)$  labeled by  $L$  and  $(z_b, z_c)$  labeled by  $H$  in the redshift axis. Shape of the region 1 and 2 is arbitrary. For those regions, we can further define four regions as it is schematically described in Fig. 1. For instance, “1,  $L$ ” stands for the region whose projection onto the mass plane coincides with the region 1 and projection onto the redshift axis coincides with  $(z_a, z_b)$ . Then, the expected number of the merger events in this region is given by

$$N_{1,L} = \int_{z_a}^{z_b} \int_{\text{region1}} dN. \quad (2.2)$$

The expected number in the other regions can be expressed in a similar manner. If the merger rate density takes the separable form (1.1), by substituting Eq. (2.1), we obtain

$$\begin{aligned} N_{1,L} &= \int_{z_a}^{z_b} \int_{\text{region1}} \mathcal{R}(M, q, z) \frac{T}{1+z} \frac{4\pi r^2(z) dz}{H(z)} \frac{M}{(1+q)^2} dM dq \\ &= T \mathcal{R}_0 \left[ \int_{z_a}^{z_b} \frac{4\pi r^2(z)}{(1+z)} \frac{f(z)}{H(z)} dz \right] \times \left[ \int_{\text{region1}} \frac{M}{(1+q)^2} h(M, q) dM dq \right]. \end{aligned} \quad (2.3)$$

It then follows that a ratio defined by

$$R_A \equiv \frac{N_{A,H}}{N_{A,L}} = \int_{z_b}^{z_c} \frac{4\pi r^2(z)}{(1+z)} \frac{f(z)}{H(z)} dz \bigg/ \int_{z_a}^{z_b} \frac{4\pi r^2(z)}{(1+z)} \frac{f(z)}{H(z)} dz \quad (2.4)$$

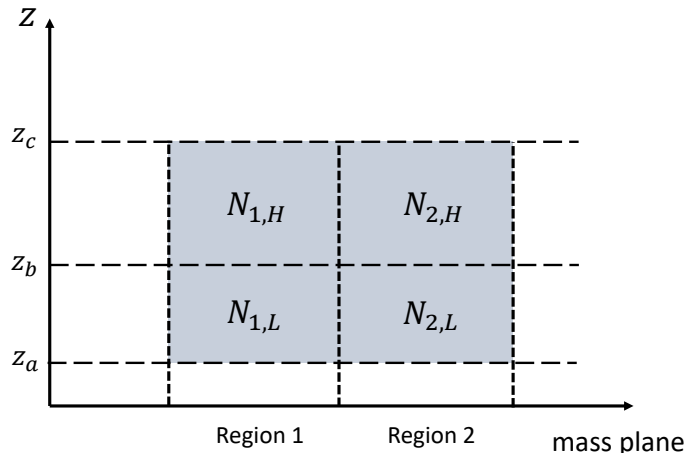


Figure 1: Definition of the division of the  $(M, q, z)$  subspace into four regions. The horizontal axis represents the two-dimensional mass plane.

becomes independent of  $A$ , where  $A$  stands for either 1 or 2. Taking contraposition of this statement, we can state that if the ratio  $R_A$  depends on  $A$ , the merger rate does not take the separable form like Eq. (1.1). Therefore, the hypothesis that the time dependence of the merger rate density is independent of the BH masses can be tested by checking whether the ratio  $R_A$  is independent of  $A$  or not, which is the basic idea underlying the following analysis.

## 2.2 Hypothesis testing

Having explained the basic idea, we formulate the statistical test of if the merger rate density takes the separable form given by Eq. (1.1) or not. We do this by the hypothesis testing. For technical convenience, instead of  $R_A$ , we will use a different quantity defined by  $p_A \equiv \frac{N_{A,H}}{N_{A,L} + N_{A,H}} = \frac{R_A}{1 + R_A}$  in the following analysis. Given that there is one-to-one correspondence between  $p_A$  and  $R_A$ , the use of  $p_A$  is not essentially better than  $R_A$ . Based on the discussion in the previous subsection, the merger rate density with the separable form leads to a relation  $p_1 = p_2$ . This is the mathematical expression that is suitable and ready for making the statistical test we want to conduct. Since we aim to clarify if the time evolution of the merger rate density is independent of the BH masses, we choose our null hypothesis  $H_0$  to be

$$H_0 : p_1 = p_2 \tag{2.5}$$

and alternative hypothesis  $H_1$  as

$$H_1 : p_1 \neq p_2. \tag{2.6}$$

In what follows, we will explain how to test the hypothesis  $H_0$ .

We use lower-case letter  $n$  to denote the number of the sample merger events in each subregion introduced in the previous subsection (see also Fig. 1). For instance, the number of the events in the region A ( $A = 1, 2$ ) in  $(z_a, z_b)$  is  $n_{A,L}$  (same for the others). Then,  $n_{A,H}$  obeys the binomial distribution  $\text{Bin}(n_A, p_A)$ , where  $n_A \equiv n_{A,L} + n_{A,H}$  is the sample size in the region A. For large sample size, which is the assumption we are going to make, this distribution is well approximated by the normal distribution, i.e.,  $\text{Bin}(n_A, p_A) \approx N(n_A p_A, n_A p_A(1 - p_A))$ . Thus, a statistical quantity  $\bar{p}_A \equiv \frac{n_{A,H}}{n_A}$  obeys the normal distribution  $N(p_A, p_A(1 - p_A)/n_A)$ .

Now, under the assumption that the hypothesis  $H_0$  is true, a test statistic  $T_{\text{stat}}$  defined by

$$T_{\text{stat}} \equiv \frac{\bar{p}_1 - \bar{p}_2}{\sqrt{\bar{p}(1 - \bar{p}) \left( \frac{1}{n_1} + \frac{1}{n_2} \right)}}, \quad (2.7)$$

where  $\bar{p} \equiv \frac{n_1 \bar{p}_1 + n_2 \bar{p}_2}{n_1 + n_2}$  is the pooled population proportion, obeys the normal distribution  $N(0, 1)$ . Thus, we can / (can not) reject the hypothesis  $H_0$  at a significance level  $\alpha$  by computing whether  $|T_{\text{stat}}|$  is larger/smaller than  $\sqrt{2} \text{Erfc}^{-1}(\alpha)$  (two-tailed test), where  $\text{Erfc}(x) \equiv \frac{2}{\sqrt{\pi}} \int_x^\infty e^{-t^2} dt$  is the complementary error function. This is our main strategy of our statistical test.

In order to have a rough idea of how much the above mentioned method works for testing the merger rate density given by Eq. (1.1), let us crudely estimate the required sample size to reject the hypothesis  $H_0$  at the 5 % significance level for the case where the merger rate density does not take the separable form. To this end, we do a simple parametrization for such a case by  $p_1 - p_2 = \Delta p$  ( $\neq 0$ ). The factor in the denominator  $\sqrt{\bar{p}(1 - \bar{p})}$  takes the maximum at  $\bar{p} = \frac{1}{2}$ , and we choose the value  $\sqrt{\bar{p}(1 - \bar{p})} = \frac{1}{2}$  which minimizes  $T_{\text{stat}}$  when other parameters are fixed. Replacing  $\bar{p}_1 - \bar{p}_2$  appearing in the numerator of Eq. (2.7) by  $\Delta p$  as a representative value, the hypothesis  $H_0$  is rejected for  $|\Delta p| > 0.98 \sqrt{\frac{1}{n_1} + \frac{1}{n_2}}$ . The right-hand side of this condition becomes minimum at  $n_1 = n_2$  for a fixed  $n = n_1 + n_2$ . Thus, the minimum sample size  $n$  needed to reject  $H_0$  for the merger rate density parametrized by  $\Delta p$  is at least about  $3.84/(\Delta p)^2$ .

### 3 Demonstration

In this section, we demonstrate the statistical approach introduced in the previous section by studying the distribution of  $T_{\text{stat}}$  of the samples for some specific merger rate densities. By doing this, we are able to have a prospect for the effectiveness of the proposed method when it is applied for the future observational data. In what follows, we study two representative cases for the merger rate density: the separable form and the non-separable form. The study of the former case allows us to confirm the robustness of the method by checking that the distribution of  $T_{\text{stat}}$  of the mock data with large sample size approximates the normal distribution  $N(0, 1)$ . This can be also used as a check of the

probability of making a type I error for the null hypothesis  $H_0$ . Meanwhile, the analysis of the latter case illustrates how efficiently the null hypothesis  $H_0$  is rejected when the alternative hypothesis  $H_1$  is true. Thus, this case provides us a good estimate of making a type II error.

As it is evident from how the statistical method is formulated, the choice of the region 1 and 2 is completely arbitrary. In the following analysis, we define these regions as

$$\text{region 1} = \{(M, q) | M \leq M_{\text{div}}, 0 \leq q \leq 1\}, \quad \text{region 2} = \{(M, q) | M > M_{\text{div}}, 0 \leq q \leq 1\}.$$

Here  $M_{\text{div}}$  is the critical total mass that divides the region 1 and 2.

### 3.1 Separable form

In this subsection, we study the merger rate density which takes the separable form (1.1). As the shape of the merger rate density, we consider two examples: the mergers of the PBH binaries and the mergers of the astrophysical BH binaries which follow the star formation rate.

#### 3.1.1 PBH mergers

As for the PBH mergers, we assume that the mass dependent part  $h(m_1, m_2)$  is given by

$$h(m_1, m_2) = C\psi(m_1)\psi(m_2), \quad (3.1)$$

where  $\psi(m)$  is the PBH mass function, and  $C$  is a normalization constant such that  $\int h(m_1, m_2)dm_1dm_2 = 1$ . The time evolution part  $f(t)$  is given by

$$f(t) = \left(\frac{t}{t_0}\right)^{-\frac{34}{37}}, \quad (3.2)$$

where  $t_0$  is the age of the Universe. This time dependence is realized for PBH binaries that formed in the radiation dominated epoch [26–28] and this formation channel dominates the PBH merger rate if the PBH binaries are not disrupted by other gravitational sources throughout their subsequent evolution [4]. The PBH mass function  $\psi(m)$  strongly depends on the models of the early universe. In this paper, we consider the log-normal shape

$$\psi(m) = \exp\left(-\frac{1}{2\sigma^2} \ln^2\left(\frac{m}{m_0}\right)\right), \quad (3.3)$$

which is a widely-used phenomenological functional form [29]. Here,  $m_0$  and  $\sigma$  are free parameters and we choose  $M_0 = 40 M_\odot$ ,  $\sigma = 0.2$  in our analysis.

The red dots in the left panel of Fig. 2 show the histogram of  $T_{\text{stat}}$  of one thousand realizations each of which has  $n_1 + n_2 = 1000$  sample size. The blue dots are the histogram of  $T_{\text{stat}}$  obeying the normal distribution  $N(0, 1)$  which, as it is discussed in the previous

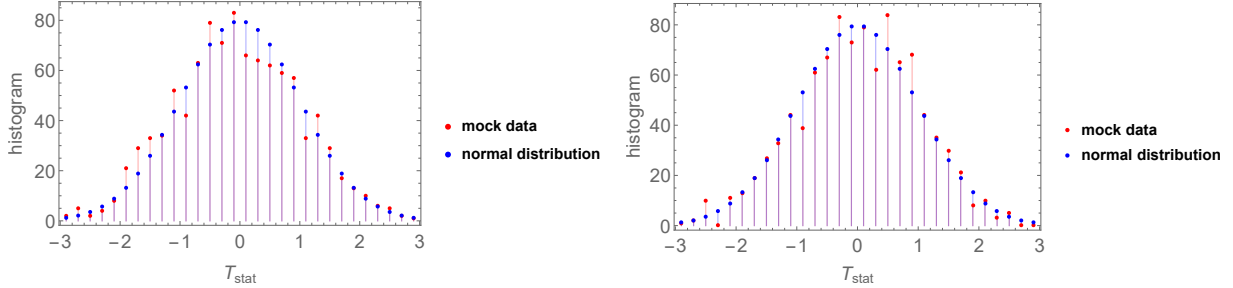


Figure 2: Histograms of  $T_{\text{stat}}$  of one thousand realizations for the merger rate density with the separable form. Each realization has  $n_1 + n_2 = 1000$  sample size. Left panel is for the PBH merger rate density, and the right panel is for the merger rate density of the astrophysical BHs. Explicit shape of the merger rate density and the underlying assumptions for each model are given in the main text.

section, should be realized if the merger rate density takes the separable form. As it is evident from the figure, the distribution of  $T_{\text{stat}}$  of the sample data is consistent with the normal distribution, which explicitly demonstrates the validity of the statistical method presented in the previous section. Our choice of parameters defining the four regions shown in Fig. 1 is  $(M_{\text{div}}, z_b, z_c) = (80 M_{\odot}, 0.5, 1.0)$ .

### 3.1.2 Mergers of astrophysical BHs

As for the shape of the merger rate density of the astrophysical BHs, we adopt the simple phenomenological model studied in [30] <sup>#3</sup>. This model is disfavored by the updated analysis presented in [31]. Nevertheless, we adopt this model in our analysis because our purpose is to demonstrate the effectiveness of our statistical method, and the use of the simple model would be enough for this purpose. It should be also noticed that there remains a possibility that only some fraction of the merger events obeys this model. The mass dependent part  $h(m_1, m_2)$  in this model is given by

$$h(m_1, m_2) = C m_1^{-\alpha} \left( \frac{m_2}{m_1} \right)^{\beta_q} \Theta(m_2 - m_{\text{min}}) \Theta(m_{\text{max}} - m_1) \Theta(m_1 - m_2), \quad (3.4)$$

where  $\Theta(x)$  is the Heaviside function, and  $C$  is the normalization constant. This shape contains four free parameters  $\alpha, \beta_q, m_{\text{min}}$ , and  $m_{\text{max}}$ . In [30], this model has been compared with the data obtained during the first and the second observing runs of LIGO and Virgo, and the posteriors of the four free parameters are derived. In our analysis, we choose them to be  $\alpha = 1.3$ ,  $\beta_q = 7$  and  $(m_{\text{min}}, m_{\text{max}}) = (8 M_{\odot}, 40 M_{\odot})$  which are consistent with the posteriors mentioned above. The time evolution part  $f(t)$  is assumed to exactly follow the

<sup>#3</sup>This model is called *model B* in [30]

star formation rate [32], namely,

$$f(z) = \frac{1}{0.997} \frac{(1+z)^{2.7}}{1 + \left(\frac{1+z}{2.9}\right)^{5.6}}. \quad (3.5)$$

Here we abuse the notation of  $f(t)$  by changing the argument from the cosmic time  $t$  to the redshift  $z$  since the star formation rate is commonly given in terms of  $z$ .

The red dots in the right panel of Fig. 2 show the histogram of  $T_{\text{stat}}$  of one thousand realizations for the model defined by (3.4) and (3.5). The sample size of each realization is the same as the case of the PBH mergers (i.e., the left panel);  $n = n_1 + n_2 = 1000$ . Our choice of parameters defining the four regions shown in Fig. 1 is  $(M_{\text{div}}, z_b, z_c) = (60 M_{\odot}, 0.5, 1.0)$ . The blue dots are the histogram of  $T_{\text{stat}}$  obeying the normal distribution  $N(0, 1)$ . As it is the same as the left panel, the distribution of  $T_{\text{stat}}$  of the sample data is consistent with the normal distribution. Thus, from the two examples, we are able to confirm that the hypothesis testing can reject the null hypothesis  $H_0$  at a given significance level  $\alpha$  if the value of  $T_{\text{stat}}$  constructed from data is larger than  $2\text{Erfc}^{-1}(\alpha)$ .

## 3.2 Non-separable form

Having checked that the probability of rejecting the null hypothesis  $H_0$  even when  $H_0$  is true is controlled by the significance level, we next investigate how likely it is not to reject the null hypothesis even when it is false.

### 3.2.1 Case 1: toy model

To this end, we first consider an extreme toy model in which the merger rate density is given by

$$\mathcal{R}(m_1, m_2, z) = \mathcal{R}_0 h(m_1, m_2) \left( \Theta(M_c - M) + (1+z)^5 \Theta(M - M_c) \right), \quad (3.6)$$

where  $h(m_1, m_2)$  is defined by Eq. (3.4) and  $M_c$  is a free parameter which we choose  $M_c = 40 M_{\odot}$ . While the merger rate of the BH binaries with  $m_1 + m_2 < M_c$  does not evolve with the redshift, that with  $m_1 + m_2 > M_c$  has a strong dependence on the redshift as  $\propto (1+z)^5$ . Thus, the merger rate density (3.6) takes the non-separable form which does not belong to the class defined by Eq. (1.1) and provides one example of the alternative hypothesis  $H_1$ .

The red dots in the left panel of Fig. 3 shows the histogram of  $T_{\text{stat}}$  of one thousand realizations of the merger rate density given by Eq. (3.6). It is clear that the distribution of  $T_{\text{stat}}$  is highly shifted to negative side and peaks at around  $T_{\text{stat}} = -4$ . Our choice of parameters defining the four regions shown in Fig. 1 is  $(M_{\text{div}}, z_b, z_c) = (40 M_{\odot}, 0.7, 1.0)$ . For this choice,  $p_1$  and  $p_2$  are found to be  $(p_1, p_2) = (0.51, 0.74)$  and

$$\int_{\text{Region1}} \mathcal{R}(m_1, m_2, t) dm_1 dm_2 dt = c_1 \int_{\text{Region1+Region2}} \mathcal{R}(m_1, m_2, t) dm_1 dm_2 dt \quad (3.7)$$

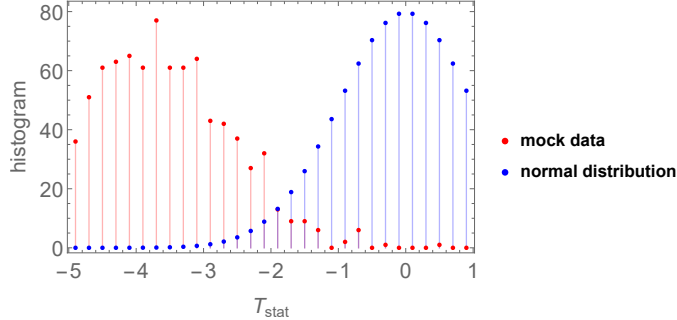


Figure 3: Histograms of  $T_{\text{stat}}$  of one thousand realizations for the merger rate density with the specific non-separable given by Eq. (3.6). Each realization has  $n_1 + n_2 = 1000$  sample size.

with  $c_1 \approx 0.055$ . Using these values as typical ones for the quantities appearing in the definition of  $T_{\text{stat}}$  (2.7), we can estimate the typical value of  $T_{\text{stat}}$  as

$$T_{\text{stat}} = -3.8 \sqrt{\frac{n}{1000}}, \quad (3.8)$$

which is consistent with the peak value of the mock data in Fig. 3.

Width of the distribution of the red dots in Fig. 3 is  $\mathcal{O}(1)$ . Actually, this does not depend on  $n$  because the typical variation of  $T_{\text{stat}}$  due to the randomness of the sampling gives a scaling  $\frac{\delta T_{\text{stat}}}{T_{\text{stat}}} \propto n^{-1/2}$  and combining it with the scaling  $T_{\text{stat}} \propto n^{1/2}$  shown in the above equation yields  $\delta T_{\text{stat}} \propto n^0$ , where the numerical value of the proportionality coefficient, which is  $\mathcal{O}(1)$ , may depend on the underlying merger rate density as well as the parameters ( $M_{\text{div}}, z_b, z_c$ ). For the current example, we find that the number of realizations yielding  $T_{\text{stat}} > -2$  out of our particular one thousand realizations is 45. Thus, if the real merger rate density is given by Eq. (3.6), we can reject the null hypothesis  $H_0$  at about the 5% significance level for the adopted parameter values when the sample size is larger than 1000.

### 3.2.2 Case 2: Mixture of the astrophysical BHs and PBHs

The above example is unrealistic in the sense that it is not based on the astrophysics and is introduced just for the purpose of demonstrating the principle of our statistical method. In the second example, we consider a less extreme case in which the merger rate is a mixture of the mergers of the astrophysical BHs and those of PBHs each of which has been separately investigated in the previous subsection. Namely, we assume the merger rate density given by

$$\mathcal{R}(m_1, m_2, t) = (1 - r)\mathcal{R}_{\text{astro}}(m_1, m_2, t) + r\mathcal{R}_{\text{PBH}}(m_1, m_2, t), \quad (3.9)$$

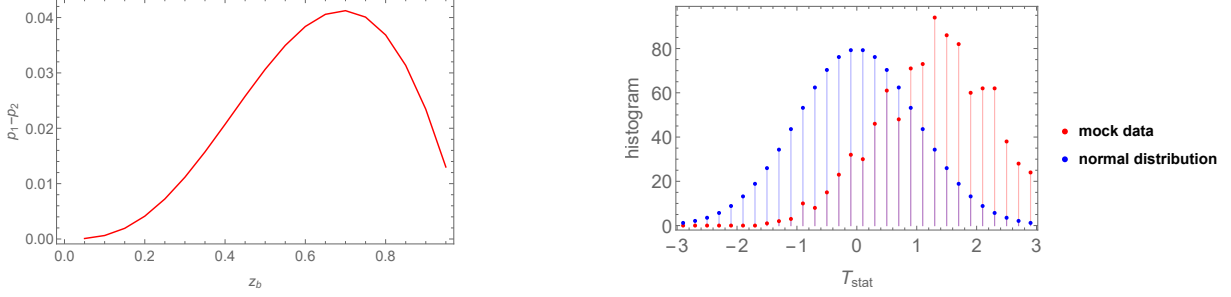


Figure 4: Left panel shows  $p_1 - p_2$  as a function of  $z_b$  with other parameters ( $M_{\text{div}}, z_c$ ) being fixed for the merger rate density given by Eq. (3.9). Right panel shows the histogram of  $T_{\text{stat}}$  of one thousand realizations for the same merger rate density as the left panel. Each realization has  $n_1 + n_2 = 1000$  sample size.

where  $\mathcal{R}_{\text{astro}}$  and  $\mathcal{R}_{\text{PBH}}$  are the merger rate density of the astrophysical BHs and PBHs introduced by Eqs. (3.1)-(3.5), respectively. Here we choose the normalization of the individual contributions such that they give the same merger rate at the present time  $t_0$ ;

$$\int \mathcal{R}_{\text{astro}}(m_1, m_2, t_0) dm_1 dm_2 = \int \mathcal{R}_{\text{PBH}}(m_1, m_2, t_0) dm_1 dm_2. \quad (3.10)$$

Thus,  $r$  denotes the fraction of the PBH contribution to the total merger rate at the present time. Since  $\mathcal{R}_{\text{astro}}$  and  $\mathcal{R}_{\text{PBH}}$  have different  $z$  dependence, the above merger rate density is non-separable for  $0 < r < 1$ .

Our choice of parameters  $M_{\text{div}}$  and  $z_c$  is  $60 M_{\odot}$  and 1.0. The left panel of Fig. 4 shows  $p_1 - p_2$  as a function of  $z_b$ . From this, we find that  $p_1 - p_2$  becomes maximal at  $z_b \approx 0.7$ . In the following analysis, we take  $z_b = 0.7$ . The right panel of Fig. 4 shows the histogram of  $T_{\text{stat}}$  of the mock data of the sample size 1000 for the merger rate density given by Eq. (3.9). The result shows that the peak of the histogram is located at about  $T_{\text{stat}} = 1.5$ . For the current merger rate density with the same values of the parameters as those adopted for generating the mock data, we find  $(p_1, p_2) \approx (0.636, 0.595)$  and

$$\int_{\text{Region1}} \mathcal{R}(m_1, m_2, t) dm_1 dm_2 dt = c_1 \int_{\text{Region1+Region2}} \mathcal{R}(m_1, m_2, t) dm_1 dm_2 dt \quad (3.11)$$

with  $c_1 \approx 0.54$ . Using these average values as typical ones for the quantities appearing in the definition of  $T_{\text{stat}}$  (2.7), we can estimate the typical value of  $T_{\text{stat}}$  as

$$T_{\text{stat}} = 1.3 \sqrt{\frac{n}{1000}} \quad (3.12)$$

in terms of the sample size  $n = n_1 + n_2$ . As expected, this value is consistent with the peak value of  $T_{\text{stat}}$  at which the histogram of  $T_{\text{stat}}$  of the mock data becomes maximal, and the width of the distribution is  $\mathcal{O}(1)$ .

To summarize, these examples demonstrate that if a given non-separable merger rate density is realized in nature, the typical value of  $T_{\text{stat}}$  given by

$$\frac{p_1 - p_2}{\sqrt{p(1-p) \left( \frac{1}{c_1} + \frac{1}{c_2} \right)}} \sqrt{n}, \quad (3.13)$$

where  $p = c_1 p_1 + c_2 p_2$  and  $c_1$  are defined by Eq. (3.7) and  $c_2 \equiv 1 - c_1$ , provides a good indicator of whether the null hypothesis  $H_0$  can be rejected or not for the data containing  $n$  merger events.

### 3.3 Effect of the measurement error of the source parameters

So far, our analysis assumed no observational errors on the parameters of the source binaries  $(M, q, z)$ . In reality, those parameters are always accompanied with the errors. Since such errors will let us mistakenly place the position of the individual merger event in the  $(M, q, z)$  space, determination of the number of the merger events in each region described in Fig. 1 is affected accordingly. As a result, the effectiveness of the hypothesis testing will be degraded to some extent. In this subsection, we evaluate the significance of the effect of the errors on the hypothesis testing.

In order to simplify our analysis, we assign 10% error randomly to the three parameters  $(M, q, z)$  of any merger events. This is not true in reality since the magnitude of the error in general depends on the binary masses and the distance to the binary. However, the following analysis based on this simplification enables us to derive a reasonable estimation on the effect of our interest and the general conclusion is that the effect is suppressed as long as the errors are much smaller than the size of the regions in Fig. 1.

As an explicit example, we again consider the merger rate density of the PBH binaries investigated in 3.1.1 with the same values of the parameters. For the binary parameters  $(M, q, z)$  of each randomly generated merger event, we multiply random number corresponding to the 10% error, namely, we change the parameters  $(M_i, q_i, z_i)$  of the  $i$ -th merger event into  $(M_i(1 + a_i), q_i(1 + b_i), z_i(1 + c_i))$ , where  $(a_i, b_i, c_i)$  are uncorrelated random numbers in the range  $[-0.1, 0.1]$ .

Fig. 5 shows the histogram of  $T_{\text{stat}}$  of one thousand realizations each of which contains  $n_1 + n_2 = 1000$  sample size. As we can see, the histogram of  $T_{\text{stat}}$  of the mock data is hardly distinguishable from that of the normal distribution. In other words, the observational errors with the current magnitude little affect the effectiveness of the hypothesis testing. Although the analytical computation of the distortion of the histogram caused by the observational errors is technically complicated, that the distortion is tiny can be formally understood in the following manner. For a given sample size  $n$ , let us evaluate the typical magnitude of the contamination to  $n_{1,L}$  due to the observational errors of  $M$  and  $z$ . Denoting that error by  $\Delta M, \Delta z$  and assuming them to be small, we find that the change

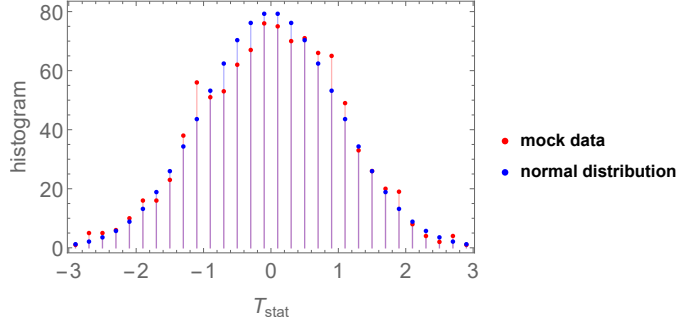


Figure 5: Histograms of  $T_{\text{stat}}$  of one thousand realizations for the merger rate density of the PBH binaries with the observational errors (10%) of the binary parameters being included. Each realization has  $n_1 + n_2 = 1000$  sample size.

of  $n_{1,L}$  is approximately given by

$$\Delta n_{1,L} \approx \frac{1}{2} \frac{\partial^2 n_{1,L}}{\partial M_b^2} (\Delta M)^2 + \frac{1}{2} \frac{\partial^2 n_{1,L}}{\partial z_b^2} (\Delta z)^2. \quad (3.14)$$

Similar results hold for  $n_{1,H}, n_{2,L}, n_{2,H}$ . This shows that  $\Delta n_{A,L}, \Delta n_{A,H}$  are parametrically suppressed by quadratic order in  $\Delta M$  and  $\Delta z$ , which demonstrates explicitly that the observational errors become negligible when both  $\Delta M$  and  $\Delta z$  are small. More precisely, given that the typical magnitude of the statistical variation of  $n_{1,L}$  is  $\sqrt{n_{1,L}}$ , the observational error may not affect the hypothesis testing as long as  $\Delta n_{1,L} \lesssim \sqrt{n_{1,L}}$  is satisfied (and also for  $n_{1,H}, n_{2,L}, n_{2,H}$ ). We have numerically confirmed that this inequality is actually fulfilled in the current example. Furthermore, if  $n_{1,L}$  is smooth and its second derivative with respect to  $M_b$  is the same order of magnitude as  $n_{1,L}/M_b^2$  (similar to  $z_b$  as well), we can derive a crude but more explicit criterion for the observational error to be negligible as

$$\frac{\Delta M}{M_b} \lesssim \frac{1}{n_{1,L}^{1/4}}, \quad \frac{\Delta z}{z_b} \lesssim \frac{1}{n_{1,L}^{1/4}}. \quad (3.15)$$

If, on the other hand,  $n_{1,L}$  sharply changes in a region involving  $M_b$  or  $z_b$ , it is possible that the observational errors significantly change the histogram of  $T_{\text{stat}}$  and impede the effectiveness of the hypothesis testing.

### 3.4 Application to the O3 data

LIGO Scientific, Virgo, and KAGRA Collaboration released the GW events taken during the third observing run (O3) as GWTC-2.1 and GWTC-3 [1, 2]. Excluding small-mass compact objects ( $< 3 M_\odot$ ) which are either BHs or neutron stars, there are 74 events which we can reasonably identify as the BH-BH merger events. At first glance, this number may look large enough to enable us to draw statistically meaningful conclusion based on our

hypothesis testing. In this subsection, we will show that the detection bias is crucial and this significantly reduces the number of the events that can be used.

In all of our analysis presented up to this stage, we have assumed that the detection probability of the merger events in the region of the parameter space defined in Fig. 1 is 1, namely, the detection probability  $p_{\text{det}}$  has been taken to be 1. This assumption is valid as long as the detection horizon of the GW detector is so large that there are sufficiently large number of the merger events which are well inside the detection horizon. This ideal situation may be achieved by the future detectors, but is hardly fulfilled in observations by the current detectors such as LIGO O3. Since, in the region where  $p_{\text{det}}$  is smaller than 1,  $p_{\text{det}}$  depends non-trivially on  $(M, q, z)$  and, in particular, takes non-separable form in general, inclusion of the merger events in the region where  $p_{\text{det}}$  is less than 1 will impede the effectiveness of the hypothesis testing. Thus, in applying our hypothesis testing to the events obtained during the O3 run, we first need to drop the merger events corresponding to value of  $p_{\text{det}}$  lower than a certain threshold.

Let us estimate this threshold value. If the events obeying the Poisson distribution are detected only with a probability  $p$  and the sample size of the detected events is  $n$ , then for the large sample size ( $n \gg 1$ ) the true number of the events is expected to be  $n/p$  with its uncertainty of our inference being about  $\sqrt{n} \frac{\sqrt{1-p}}{p}$ . Thus, we expect that the detection probability becomes a serious obstacle to our hypothesis testing if this uncertainty exceeds the Poisson fluctuation of the expected number of the true sample size  $\frac{n}{p}$  (i.e.,  $\sqrt{n/p}$ ), namely, for  $p \leq \frac{1}{2}$ . Based on this consideration, we conservatively set the threshold of  $p_{\text{det}}$  to 0.7 for which the contamination due to the selection bias is about the half of the Poisson fluctuation.

Fig. 6 shows contours of the redshift  $z_{0.7}$  at which  $p_{\text{det}}$  is equal to 0.7 in the  $M - q$  plane ( $z_{0.7} = 0.1, 0.2, 0.3, 0.4, 0.5$ ) for the LIGO-Virgo network assuming O3 run. These contours were obtained by running a public python code whose information is given in [25]. On top of the contour plot, we also superposed merger events as red circles which qualify the mentioned criterion, that is, whose redshift is less than  $z_{0.7}$  evaluated at the same position in the  $M - q$  plane. The number placed near the red circle represents the redshift of the individual event. There are 20 such events and we can then define the regions described in Fig. 1 only for those 20 events. For any choice of the boundary redshift  $z = z_c$  at our disposal, out of the above 20 events, only events which lie right to the contour  $z_{0.7} = z_c$  can be used for our statistical analysis. We found that there remain only several events after applying this selection for any value of  $z_c$ . For instance, taking  $z_c = 0.3$ , there are only seven events. Clearly, this number is too small to draw any statistical conclusion.

To summarize, this investigation shows that the number of the merger events obtained during the O3 run is not sufficient to perform the hypothesis testing to clarify if the existing GW data can already say something about the time dependence of the mass distribution of the merger rate.

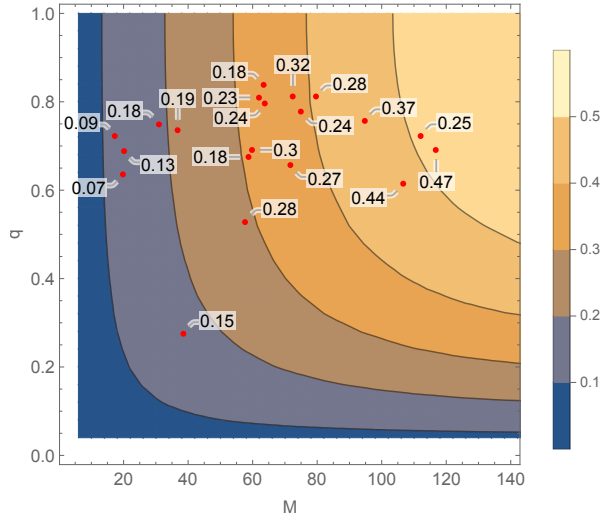


Figure 6: Contour plot of the redshift  $z_{0.7}$  on which  $p_{\text{det}} = 0.7$  assuming the sensitivity of the LIGO-Virgo O3. Red circles are the merger events whose redshift is smaller than  $z_{0.7}$ . The number placed near the red circle represents the redshift of the individual event.

## 4 Conclusions

There are several known formation channels of the binary BHs which can merge within the age of the Universe. However, due to our lack of the theoretical understanding, we are still far from predicting robustly how much each channel contributes to the total merger rate density. Generally, the fraction of each contribution depends on the BH masses as well as the merger redshift. It is known that some formation channels predict that the time dependence of the merger rate density is (exactly or nearly) independent of the BH masses. Naturally, this motivates us to investigate the statistical testing on the time independence of the mass distribution by which we may be able to obtain some clues to clarify the origin of the binary BHs. In this paper, we formulated the methodology to perform the above mentioned test and demonstrated the effectiveness of the proposed method by using the mock data.

After providing the definition of what we exactly mean by *the mass independence of the time evolution of the merger rate density*, we reformulated it into another equivalent but more convenient form for the statistical analysis. As a simple statistical test, we adopted the so-called hypothesis testing. Our null hypothesis is that the time evolution of the merger rate density does not depend on the BH masses. To test the null hypothesis, we introduced the test statistic which obeys the normal distribution  $N(0, 1)$  for the large sample size if the null hypothesis is true. In Sec. 3, by generating the mock data in two specific examples both of which satisfy the null hypothesis, we confirmed explicitly that the test statistic follows the normal distribution. We also considered two other examples in which the time evolution of the merger rate density varies for different BH masses and

showed that the central value of the test statistic deviates from zero. Analytical estimation suggests that the shift of the test statistic is proportional to the square of the sample size, and the shift of the test statistic computed from the mock data is fairly consistent with the analytical estimation. For a given merger rate density which does not fulfill the null hypothesis, this result supports reasonable estimate of the minimal sample size necessary to reject the null hypothesis. These results demonstrate the effectiveness of our hypothesis testing to determine from the (future) observational data whether the merger rate density evolves in time independently of the BH masses or not.

LIGO-Virgo-KAGRA Collaboration released more than 70 merger events detected during the O3 observing run. In order not to spoil the hypothesis testing due to the selection bias caused by the low value of the detection probability, we selected only the merger events corresponding to the detection probability above certain threshold. We found that the number of the events is not sufficient to draw any statistical conclusion and the meaningful result of our hypothesis testing can be obtained only by the future detectors having much better sensitivity.

Before closing, it should be stressed that our statistical test does not require a priori specification of the mass distribution which is largely uncertain as well as the shape of the time evolution. Thus the result of the statistical test holds valid independent of the mass distribution and the time evolution. This is in sharp contrast to previous statistical studies which derived/constrained properties of the BH mergers under specific assumptions on the mass distribution.

## Acknowledgements

We greatly appreciate Bence Kocsis for giving us useful information and suggestions. This work is supported by JST SPRING, Grant Number JPMJSP2106 (SO). This work is supported by the MEXT KAKENHI Grant Number 17H06359 (TS), JP21H05453 (TS) and the JSPS KAKENHI Grant Number JP19K03864 (TS).

## References

- [1] **LIGO Scientific, VIRGO** Collaboration, R. Abbott et al., *GWTC-2.1: Deep Extended Catalog of Compact Binary Coalescences Observed by LIGO and Virgo During the First Half of the Third Observing Run*, [arXiv:2108.01045](#).
- [2] **LIGO Scientific, VIRGO, KAGRA** Collaboration, R. Abbott et al., *GWTC-3: Compact Binary Coalescences Observed by LIGO and Virgo During the Second Part of the Third Observing Run*, [arXiv:2111.03606](#).
- [3] M. Mapelli, *Formation channels of single and binary stellar-mass black holes*, [arXiv:2106.00699](#).

- [4] M. Sasaki, T. Suyama, T. Tanaka, and S. Yokoyama, *Primordial black holes—perspectives in gravitational wave astronomy*, *Class. Quant. Grav.* **35** (2018), no. 6 063001, [[arXiv:1801.05235](#)].
- [5] I. Mandel and F. S. Broekgaarden, *Rates of Compact Object Coalescences*, [arXiv:2107.14239](#).
- [6] G. Franciolini, V. Baibhav, V. De Luca, K. K. Y. Ng, K. W. K. Wong, E. Berti, P. Pani, A. Riotto, and S. Vitale, *Quantifying the evidence for primordial black holes in LIGO/Virgo gravitational-wave data*, [arXiv:2105.03349](#).
- [7] K. Belczynski, A. Romagnolo, A. Olejak, J. Klencki, D. Chattopadhyay, S. Stevenson, M. C. Miller, J. P. Lasota, and P. A. Crowther, *The Uncertain Future of Massive Binaries Obscures the Origin of LIGO/Virgo Sources*, [arXiv:2108.10885](#).
- [8] S. Vitale, W. M. Farr, K. Ng, and C. L. Rodriguez, *Measuring the star formation rate with gravitational waves from binary black holes*, *Astrophys. J. Lett.* **886** (2019), no. 1 L1, [[arXiv:1808.00901](#)].
- [9] M. Dominik, K. Belczynski, C. Fryer, D. E. Holz, E. Berti, T. Bulik, I. Mandel, and R. O’Shaughnessy, *Double Compact Objects II: Cosmological Merger Rates*, *Astrophys. J.* **779** (2013) 72, [[arXiv:1308.1546](#)].
- [10] A. Tanikawa, T. Yoshida, T. Kinugawa, A. A. Trani, T. Hosokawa, H. Susa, and K. Omukai, *Merger rate density of binary black holes through isolated Population I, II, III and extremely metal-poor binary star evolution*, [arXiv:2110.10846](#).
- [11] C. L. Rodriguez and A. Loeb, *Redshift Evolution of the Black Hole Merger Rate from Globular Clusters*, *Astrophys. J. Lett.* **866** (2018), no. 1 L5, [[arXiv:1809.01152](#)].
- [12] C. L. Rodriguez, S. Chatterjee, and F. A. Rasio, *Binary Black Hole Mergers from Globular Clusters: Masses, Merger Rates, and the Impact of Stellar Evolution*, *Phys. Rev. D* **93** (2016), no. 8 084029, [[arXiv:1602.02444](#)].
- [13] C. L. Rodriguez, P. Amaro-Seoane, S. Chatterjee, K. Kremer, F. A. Rasio, J. Samsing, C. S. Ye, and M. Zevin, *Post-Newtonian Dynamics in Dense Star Clusters: Formation, Masses, and Merger Rates of Highly-Eccentric Black Hole Binaries*, *Phys. Rev. D* **98** (2018), no. 12 123005, [[arXiv:1811.04926](#)].
- [14] J. Samsing, D. J. D’Orazio, K. Kremer, C. L. Rodriguez, and A. Askar, *Single-single gravitational-wave captures in globular clusters: Eccentric deci-Hertz sources observable by DECIGO and Tian-Qin*, *Phys. Rev. D* **101** (2020), no. 12 123010, [[arXiv:1907.11231](#)].

- [15] L. Gondán, B. Kocsis, P. Raffai, and Z. Frei, *Eccentric Black Hole Gravitational-Wave Capture Sources in Galactic Nuclei: Distribution of Binary Parameters*, *Astrophys. J.* **860** (2018), no. 1 5, [[arXiv:1711.09989](#)].
- [16] A. Rasskazov and B. Kocsis, *The rate of stellar mass black hole scattering in galactic nuclei*, *Astrophys. J.* **881** (2019), no. 1 20, [[arXiv:1902.03242](#)].
- [17] L. Gondán and B. Kocsis, *High eccentricities and high masses characterize gravitational-wave captures in galactic nuclei as seen by Earth-based detectors*, *Mon. Not. Roy. Astron. Soc.* **506** (2021), no. 2 1665–1696, [[arXiv:2011.02507](#)].
- [18] S. Chatterjee, C. L. Rodriguez, V. Kalogera, and F. A. Rasio, *Dynamical Formation of Low-Mass Merging Black Hole Binaries like GW151226*, *Astrophys. J. Lett.* **836** (2017), no. 2 L26, [[arXiv:1609.06689](#)].
- [19] Y. Yang, I. Bartos, Z. Haiman, B. Kocsis, S. Márka, and H. Tagawa, *Cosmic Evolution of Stellar-mass Black Hole Merger Rate in Active Galactic Nuclei*, *Astrophys. J.* **896** (2020), no. 2 138, [[arXiv:2003.08564](#)].
- [20] B. Kocsis, T. Suyama, T. Tanaka, and S. Yokoyama, *Hidden universality in the merger rate distribution in the primordial black hole scenario*, *Astrophys. J.* **854** (2018), no. 1 41, [[arXiv:1709.09007](#)].
- [21] M. Raidal, C. Spethmann, V. Vaskonen, and H. Veermäe, *Formation and evolution of primordial black hole binaries in the early universe*, *Journal of Cosmology and Astroparticle Physics* **2019** (Feb, 2019) 018–018.
- [22] M. Fishbach, D. E. Holz, and W. M. Farr, *Does the Black Hole Merger Rate Evolve with Redshift?*, *Astrophys. J. Lett.* **863** (2018), no. 2 L41, [[arXiv:1805.10270](#)].
- [23] M. Fishbach, Z. Doctor, T. Callister, B. Edelman, J. Ye, R. Essick, W. M. Farr, B. Farr, and D. E. Holz, *When Are LIGO/Virgo’s Big Black Hole Mergers?*, *Astrophys. J.* **912** (2021), no. 2 98, [[arXiv:2101.07699](#)].
- [24] **LIGO Scientific, VIRGO, KAGRA** Collaboration, R. Abbott et al., *The population of merging compact binaries inferred using gravitational waves through GWTC-3*, [arXiv:2111.03634](#).
- [25] H.-Y. Chen, D. E. Holz, J. Miller, M. Evans, S. Vitale, and J. Creighton, *Distance measures in gravitational-wave astrophysics and cosmology*, *Class. Quant. Grav.* **38** (2021), no. 5 055010, [[arXiv:1709.08079](#)].
- [26] T. Nakamura, M. Sasaki, T. Tanaka, and K. S. Thorne, *Gravitational waves from coalescing black hole MACHO binaries*, *Astrophys. J. Lett.* **487** (1997) L139–L142, [[astro-ph/9708060](#)].

- [27] K. Ioka, T. Chiba, T. Tanaka, and T. Nakamura, *Black hole binary formation in the expanding universe: Three body problem approximation*, *Phys. Rev. D* **58** (1998) 063003, [[astro-ph/9807018](#)].
- [28] M. Sasaki, T. Suyama, T. Tanaka, and S. Yokoyama, *Primordial Black Hole Scenario for the Gravitational-Wave Event GW150914*, *Phys. Rev. Lett.* **117** (2016), no. 6 061101, [[arXiv:1603.08338](#)]. [Erratum: *Phys.Rev.Lett.* 121, 059901 (2018)].
- [29] B. Carr, M. Raidal, T. Tenkanen, V. Vaskonen, and H. Veermäe, *Primordial black hole constraints for extended mass functions*, *Phys. Rev. D* **96** (2017), no. 2 023514, [[arXiv:1705.05567](#)].
- [30] **LIGO Scientific, Virgo** Collaboration, B. P. Abbott et al., *Binary Black Hole Population Properties Inferred from the First and Second Observing Runs of Advanced LIGO and Advanced Virgo*, *Astrophys. J. Lett.* **882** (2019), no. 2 L24, [[arXiv:1811.12940](#)].
- [31] **LIGO Scientific, Virgo** Collaboration, R. Abbott et al., *Population Properties of Compact Objects from the Second LIGO-Virgo Gravitational-Wave Transient Catalog*, *Astrophys. J. Lett.* **913** (2021), no. 1 L7, [[arXiv:2010.14533](#)].
- [32] P. Madau and M. Dickinson, *Cosmic Star Formation History*, *Ann. Rev. Astron. Astrophys.* **52** (2014) 415–486, [[arXiv:1403.0007](#)].